

## New data and the hard pomeron

A Donnachie  
Department of Physics, Manchester University

P V Landshoff  
DAMTP, Cambridge University\*

### Abstract

New structure-function data are in excellent agreement with the existence of a hard pomeron, with intercept about 1.4. It gives a very economical description of the data. Having fixed 2 parameters from the data for the real-photon cross section  $\sigma^{\gamma p}$ , we need just 5 further parameters to fit the data for  $F_2(x, Q^2)$  with  $x \leq 0.001$ . The available data range from  $Q^2 = 0.045$  to  $35 \text{ GeV}^2$ . With guesses consistent with dimensional counting for the  $x$  dependences of our three separate terms, the fit extends well to larger  $x$  and to  $Q^2 = 5000 \text{ GeV}^2$ . With no additional parameters, it gives a good description of data for the charm structure function  $F_2^c(x, Q^2)$  from  $Q^2 = 0$  to  $130 \text{ GeV}^2$ . The two pomerons also give a good description of both the  $W$  and the  $t$  dependence of  $\gamma p \rightarrow J/\psi p$ .

In previous papers, we have shown that the Regge approach provides a very good description<sup>[1]</sup> of the data on the small- $x$  behaviour of the proton structure function  $F_2(x, Q^2)$ , on<sup>[2]</sup> the charm structure function  $F_2^c(x, Q^2)$ , and on<sup>[3]</sup> exclusive photoproduction of the  $J/\psi$ . These data call for a new Regge trajectory, whose intercept is about 1.4, which we call the hard pomeron. In conformity with traditional Regge theory<sup>[4]</sup> the hard-pomeron has an intercept that does not vary with  $Q^2$ , but its contribution is added to that of the soft pomeron and, because their relative weight is  $Q^2$ -dependent, their combined effect is similar to that of a single  $Q^2$ -dependent trajectory. The conventional theory of perturbative evolution appears rather to favour a genuinely  $Q^2$ -dependent trajectory; however, we have explained<sup>[5]</sup> that the way in which the evolution is usually applied is not valid at small  $x$ . Resummation is known to be necessary and to have a very significant effect, but at present we do not have adequate knowledge to implement it.

Because of this, it is important to study data, to try and extract whatever theoretical message they may contain. Fits with huge numbers of parameters are unlikely to reveal such messages at all clearly, but the Regge approach has the merit that it requires rather few parameters. There have recently appeared new and more accurate data<sup>[6]</sup> for  $F_2(x, Q^2)$  at small  $Q^2$  from ZEUS and<sup>[7]</sup> at larger values of  $Q^2$  from H1, who have also finalised<sup>[8]</sup> their data on exclusive  $J/\psi$  photoproduction. In this paper we confront these new measurements with the Regge approach, and find that it stands up well.

Our previous fit<sup>[1]</sup> to the data for  $F_2(x, Q^2)$  used simple powers of  $x$ :

$$F_2(x, Q^2) = \sum_{i=0}^2 f_i(Q^2) x^{-\epsilon_i} \quad (1)$$

---

\* email addresses: ad@a35.ph.man.ac.uk, pvl@damtp.cam.ac.uk

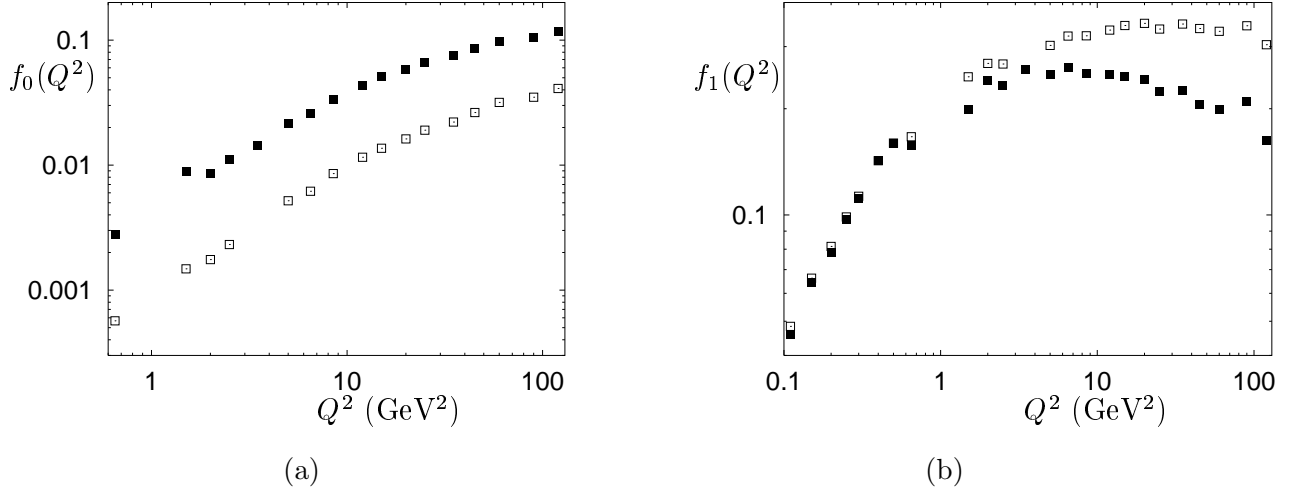


Figure 1: The coefficient functions  $f_i(Q^2)$  of (1) extracted from the new data<sup>[6,7]</sup>, (a) for the hard pomeron and (b) for the soft. The points are for  $\epsilon_0 = 0.36$  (black points) and 0.5 (open points).

Here, the  $i = 0$  term is hard-pomeron exchange,  $i = 1$  is soft-pomeron exchange, and  $i = 2$  is  $(f_2, a_2)$  exchange. Our fit extended up to  $x = 0.07$ . However, the new data are so very accurate, with errors just a few percent, that it is no longer safe to go to such large  $x$  with simple powers: they will be modified by unknown factors which eventually ensure that  $F_2(x, Q^2)$  vanishes at each  $Q^2$  when  $x \rightarrow 1$ . The dimensional-counting rules would require both the soft and the hard pomeron contributions to behave near  $x = 1$  as  $(1 - x)^7$ , and the  $(f_2, a_2)$  contribution as  $(1 - x)^3$ , but it is not clear that these rules are valid and there is no theoretical information about how the factors should behave away from  $x = 1$ . Nevertheless, we make simple guesses, which conform with the dimensional-counting rules, and which are probably a better approximation than omitting the factors altogether:

$$F_2(x, Q^2) = f_0(Q^2) x^{-\epsilon_0} (1 - x)^7 + f_1(Q^2) x^{-\epsilon_1} (1 - x)^7 + f_2(Q^2) x^{-\epsilon_2} (1 - x^2)^3 \quad (2)$$

We explain below our reason for using  $(1 - x^2)^3$  for the  $(f_2, a_2)$  term, rather than simply  $(1 - x)^3$ . Our fit uses only data up to  $x = 0.001$ , where the factors have less than 1% effect, but we will find that we have quite good agreement with the data even beyond  $x = 0.07$ , where they are rather important.

As we have done before<sup>[1]</sup>, we fix the soft-pomeron power  $\epsilon_1$  at the value 0.0808 which we found<sup>[9]</sup> from data for  $\sigma^{pp}$  and  $\sigma^{\bar{p}p}$ , though it has been argued<sup>[10]</sup> that a rather larger value should be taken, perhaps 0.093. There is little theoretical understanding of the functions  $f_1(Q^2)$  in (1). All we know is that near  $Q^2 = 0$

$$f_i(Q^2) \sim X_i (Q^2)^{1+\epsilon_i} \quad (3)$$

To guide us on the likely functional forms of the coefficient functions we extract their values at each  $Q^2$  for which there are new data<sup>[6,7]</sup> for  $F_2(x, Q^2)$ . In order to have enough data points at each  $Q^2$  we include values of  $x$  up to 0.02, rather than the up to 0.001 as we have suggested above. Even up to  $x = 0.02$  the contribution from the  $(f_2, a_2)$  term is small, so we omit it at this stage; that is, we use (2) without the last term. Figure 1 shows the coefficient functions  $f_0(Q^2)$  and  $f_1(Q^2)$  corresponding to two choices of the hard-pomeron power,  $\epsilon_0 = 0.36$  and  $\epsilon_0 = 0.50$ , which lie either side of the value  $\epsilon_0 = 0.44$  which we have recently said<sup>[2]</sup> is preferred. We stress that these fits should not be taken too seriously: we use them only as a guide and then go back to the beginning with the fitting.

By making a rough fit to the points in figure 1a we may deduce that the shape of the hard-pomeron

coefficient  $f_0(Q^2)$  is likely to be well-described by the form

$$f_0(Q^2) = X_0 \left( \frac{Q^2}{1 + Q^2/Q_0^2} \right)^{1+\epsilon_0} (1 + Q^2/Q_0^2)^{\epsilon_0/2} \quad (4a)$$

We introduced this form in our fit<sup>[2]</sup> to the data on the charm structure function  $F_2^c(x, Q^2)$ . It is more economical than the shape we used originally<sup>[1]</sup>, in that it includes one fewer parameter. Figure 1b shows that the shape of the soft-pomeron coefficient function  $f_1(Q^2)$  is sensitive to the value for the hard-pomeron power  $\epsilon_0$ . Our previous fits suggested that  $f_1(Q^2)$  goes to zero at large  $Q^2$ , but we find now that we obtain a good fit with a form that contains one fewer parameter and obeys Bjorken scaling at large  $Q^2$ :

$$f_1(Q^2) = X_1 \left( \frac{Q^2}{1 + Q^2/Q_1^2} \right)^{1+\epsilon_1} \quad (4b)$$

Our fit uses data for  $F_2(x, Q^2)$  with  $x \leq 0.001$ , where the contribution from  $f_2$  and  $a_2$  exchange is small, less than 5% according to our results. However, we include also data for the real-photon total cross section  $\sigma^{\gamma p}$ , the very accurate pre-HERA data with  $6 < W < 18$  GeV. For these data  $f_2$  and  $a_2$  exchange is important. We use the value we have previously<sup>[9]</sup> taken for the  $(f_2, a_2)$  intercept,  $1 + \epsilon_2$  with  $\epsilon_2 = -0.4525$ . For want of adequate information, we assume that the corresponding coefficient function is similar in form to (4):

$$f_2(Q^2) = X_2 \left( \frac{Q^2}{1 + Q^2/Q_2^2} \right)^{1+\epsilon_2} \quad (4c)$$

Then

$$\sigma^{\gamma p}(\nu) = \frac{4\pi^2\alpha}{Q^2} F_2(Q^2/2\nu, Q^2) \Big|_{Q^2=0} = 4\pi^2\alpha \sum_{i=0}^2 X_i (2\nu)^{\epsilon_i} \quad (5)$$

We use (2), (4) and (5), with  $\epsilon_0, X_0, Q_0^2, X_1, Q_1^2, X_2$  and  $Q_2^2$  as free parameters, to perform a least-squares fit to the new ZEUS and H1 data for  $F_2(x, Q^2)$  up to  $x = 0.001$ , together with the data for  $\sigma^{\gamma p}$ . The best values are

$$\epsilon_0 = 0.4372 \quad X_0 = 0.001461 \quad Q_0^2 = 9.108 \quad X_1 = 0.5954 \quad Q_1^2 = 0.5894 \quad X_2 = 1.154 \quad Q_2^2 = 0.2305 \quad (6)$$

and the average  $\chi^2$  for each of the 148 data points is 0.98. In making our fit, we combine the statistical and systematic errors in quadrature. In the case of the new H1 data, we ignore the correlated errors. Figure 2 shows the data we have used, together with the fits.

We make a number of comments on these fits:

**1** Because the errors on the data are so small, the  $\chi^2$  per data point is very sensitive to the precise values of the parameters (6). However, it should not be thought that the parameters are determined to anything like the quoted accuracy: one can change any of them, with compensating changes to the others, and still achieve a good  $\chi^2$ . Furthermore, by completely ignoring the correlated errors in the H1 data we have been much too conservative. So the error on the value of  $\epsilon_0$  is at least 10%.

**2** The real-photon cross section  $\sigma^{\gamma p}$  plays an important role in the fit and determines the values of the parameters  $X_1$  and  $X_2$ . Without these data,  $\epsilon_0$  could vary over a large range, from less than 0.25 to

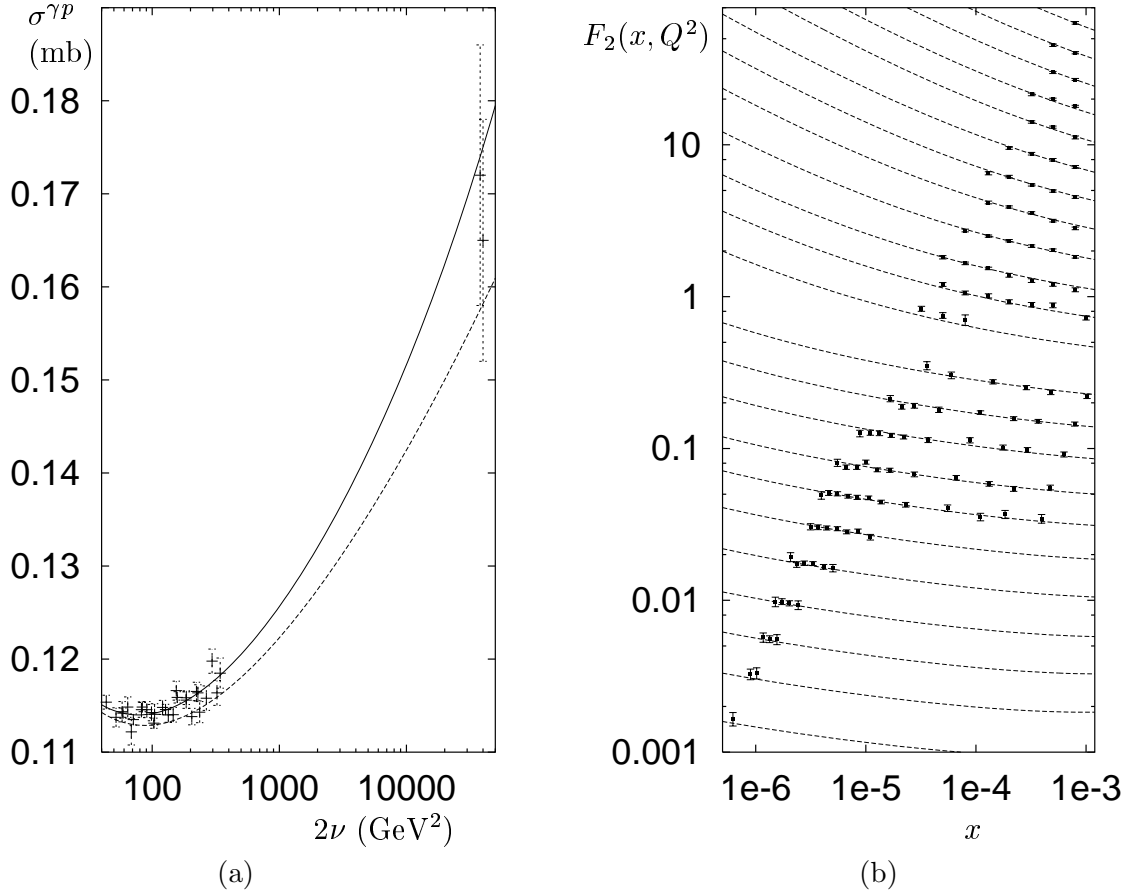


Figure 2: The fit described in the text to (a) the real-photon cross section  $\sigma^{\gamma p}$  and (b) to recent ZEUS and H1 data<sup>[6,7]</sup> for  $F_2(x, Q^2)$ . In (a) the lower line omits the contribution from hard-pomeron exchange. In (b), the data for the different values of  $Q^2$  have been scaled with powers of  $\sqrt{2}$ ;  $Q^2$  varies from 0.045 GeV<sup>2</sup> at the bottom to 35 GeV<sup>2</sup> at the top.

more than 0.5, with the appropriate change of shape for the soft-pomeron coefficient function  $f_1(Q^2)$  suggested by figure 1a, and still give a good  $\chi^2$ . The values of the  $X_i$  in (6) correspond to

$$\sigma^{\gamma p} = 0.00016 (2\nu)^{\epsilon_0} + 0.067 (2\nu)^{\epsilon_1} + 0.129 (2\nu)^{\epsilon_2} \quad (7)$$

in mb units with  $\nu$  in GeV<sup>2</sup>. The values 0.067 and 0.129 for the soft-pomeron and  $f_2, a_2$  coefficients are the same as in our original fit<sup>[9]</sup> without a hard-pomeron term. This is because, as is evident from figure 2a, where the lower curve omits the hard-pomeron term in (7), the hard-pomeron contribution is small at  $Q^2 = 0$  in the energy range of the pre-HERA data, smaller than we had it previously<sup>[1]</sup> but not completely negligible. We have explained before<sup>[5]</sup> that the question whether the hard-pomeron term is present already at  $Q^2 = 0$  is of considerable theoretical importance. If it is present then the hard pomeron is not, as many people think, generated by perturbative evolution, though the observed increase with  $Q^2$  of its importance may be a consequence of perturbative evolution.

**3** We have previously noted<sup>[2]</sup> that the charm structure function  $F_2^c(x, Q^2)$  is well described by hard-pomeron exchange alone, and that hard-pomeron exchange seems to be flavour blind even at low  $Q^2$ . Figure 3a shows ZEUS data<sup>[11]</sup> together with  $\frac{2}{5}$  of the hard-pomeron contribution to the complete  $F_2(x, Q^2)$  used in figure 2b. The fraction  $\frac{2}{5}$  is  $e_c^2/(e_u^2 + e_d^2 + e_s^2 + e_c^2)$ . This zero-parameter fit works

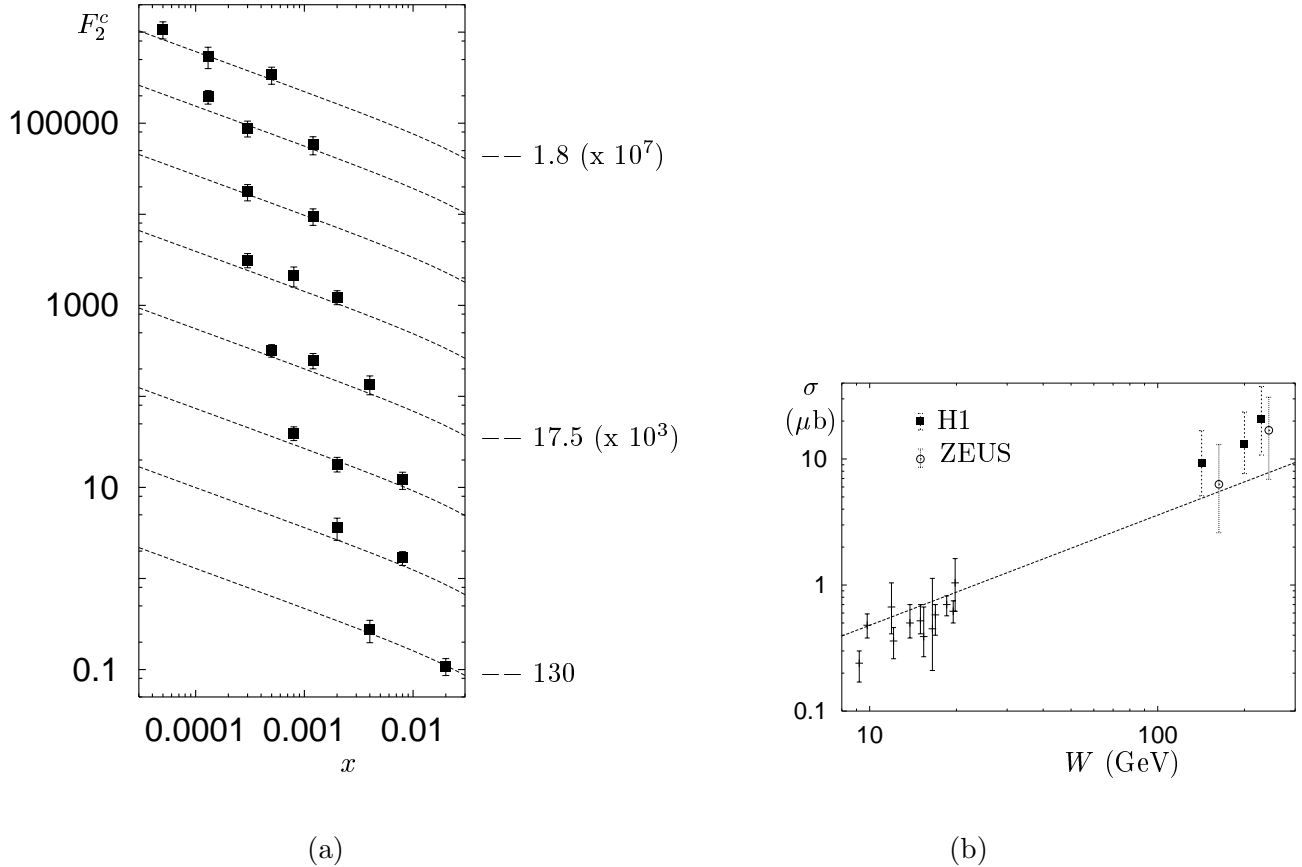


Figure 3: (a) ZEUS data<sup>[11]</sup> for the charm structure function with the zero-parameter hard-pomeron fit. The data for the various values of  $Q^2$  have been scaled with powers of 10, with  $Q^2 = 1.8 \text{ GeV}^2$  at the top and  $130 \text{ GeV}^2$  at the bottom. (b) data for the charm photoproduction cross section; the fit is that shown in (a), extrapolated to  $Q^2 = 0$ .

well all the way from  $Q^2 = 1.8$  to  $130 \text{ GeV}^2$ . It even continues to be satisfactory when extrapolated to  $Q^2 = 0$ : see figure 3b.

4 We may check that the values of  $X_2$  and  $Q_2^2$  in (6) are consistent with data for real and virtual photons scattering on a neutron target. These parameters relate to the sum of  $f_2$  and  $a_2$  exchange. When we switch to a neutron target, the contribution from  $a_2$  exchange changes sign. So the difference  $F_2^p(x, Q^2) - F_2^n(x, Q^2)$ , which has been measured by the EMC collaboration<sup>[12]</sup>, corresponds just to  $a_2$  exchange. We assume that the  $Q^2$  dependence of  $f_2$  and  $a_2$  exchanges have the same shape, that is both are given by (4c) with the same value for  $Q_2^2$ , given in (6). The  $x$  dependence of the data is well described by including a factor  $(1 - x^2)^3$ , which is what led us to the choice of the last term in (2). With such a factor, we fit the  $(p - n)$  data with a  $\chi^2$  of 0.82 per data point, with

$$X_2^{p-n} = 0.37 \quad (8)$$

This corresponds to  $a_2$  exchange having about  $\frac{1}{5}$  the strength of  $f_2$  exchange. The  $Q^2$  values of the EMC data vary between 7 and  $170 \text{ GeV}^2$ . We assume that this factor of  $\frac{1}{5}$  remains valid down to  $Q^2 = 0$ . In figure 4a the fit (7) is extrapolated to low energies and is compared with the data for  $\sigma^{\gamma p}$ . In figure 4b the data are for  $\sigma^{\gamma n}$  and the upper curve is the same fit, while the lower curve has the coefficient of the last term multiplied by  $\frac{2}{3}$ . This lower value corresponds to the contribution from

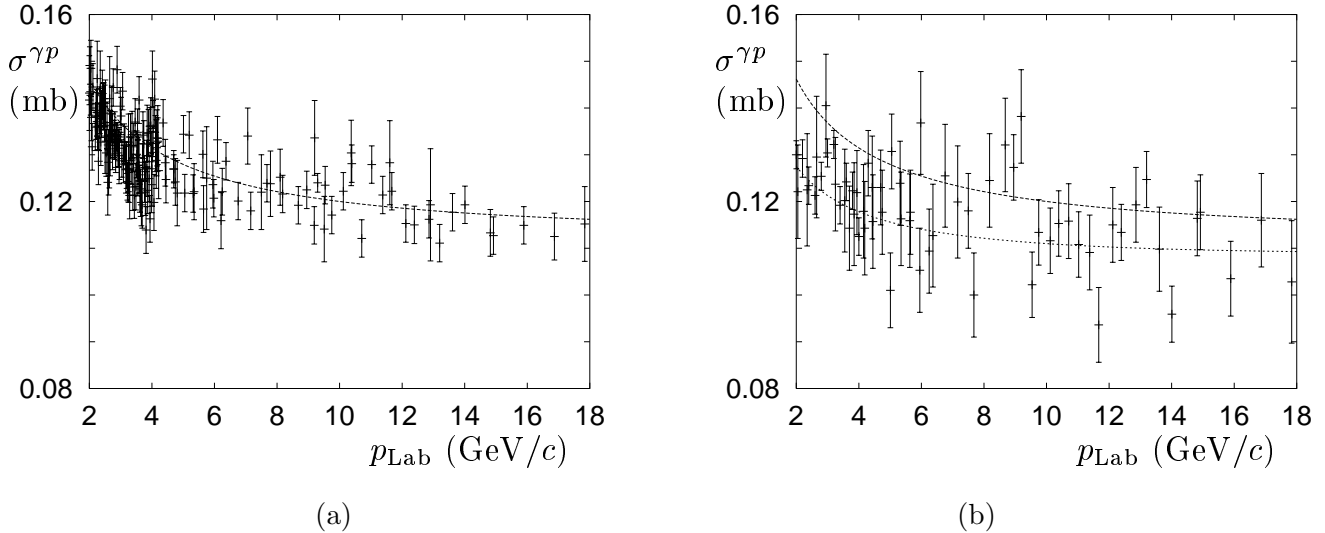


Figure 4: Data for (a)  $\sigma^{\gamma p}$  and (b)  $\sigma^{\gamma n}$ . The curve in (a) and the upper curve in (b) is the fit (7); the lower curve in (b) has the last term reduced by a factor  $\frac{2}{3}$ .

$a_2$  exchange to  $\sigma^{\gamma p}$  being  $\frac{1}{5}$  that of  $f_2$  exchange. It gives a reasonable eyeball fit and it provides a consistency check.

**5** We have previously shown that a combination of soft and hard pomeron exchange gives a good description of the differential cross section for the exclusive process  $\gamma p \rightarrow J/\psi p$ . The preliminary data on which we based our fit<sup>[2]</sup> have now been finalised<sup>[8]</sup>. We fit the data assuming that the amplitude is

$$A(s, t) = i \sum_{i=0,1} \beta_i(t) (\alpha'_i s)^{e_i(t)} e^{-\frac{1}{2} i \pi e_i(t)} \quad (9)$$

Here,  $1 + e_i(t)$  are the two pomeron trajectories, so that  $e_i(0) = \epsilon_i$ . We assume that both are linear, and call their slopes  $\alpha'_i$ . Before we raise  $s$  to the power  $e_i(t)$  we need to divide it by a squared-mass scale to make it dimensionless. We decided long ago<sup>[13]</sup> that it was appropriate to use  $1/\alpha'_i$  for each power. We found also<sup>[2]</sup>, when considering the preliminary data from H1, that the data were well described by assuming that the coupling functions are

$$\beta_i(t) = b_i F_1(t) \quad (10)$$

with  $b_i$  constants and  $F_1(t)$  the Dirac elastic form factor of the proton:

$$F_1(t) = \frac{4m^2 - 2.79t}{4m^2 - t} \frac{1}{(1 - t/0.71)^2} \quad (11)$$

where  $m$  is the proton mass. It is known<sup>[13]</sup> that the coupling of the soft pomeron to the proton varies as  $F_1(t)$  and it is reasonable to assume that the same is true for the hard pomeron. So in using (11) we are assuming that each pomeron has constant coupling to the  $\gamma$ - $J/\psi$  vertex. The phases  $e^{-\frac{1}{2} i \pi e_i(t)}$  are the standard Regge phases. The value of the soft-pomeron slope is well established<sup>[13]</sup> to be  $0.25 \text{ GeV}^{-2}$ . For the hard-pomeron slope we take the same value as we have used before,

$$\alpha'_0 = 0.1 \text{ GeV}^{-2} \quad (12)$$

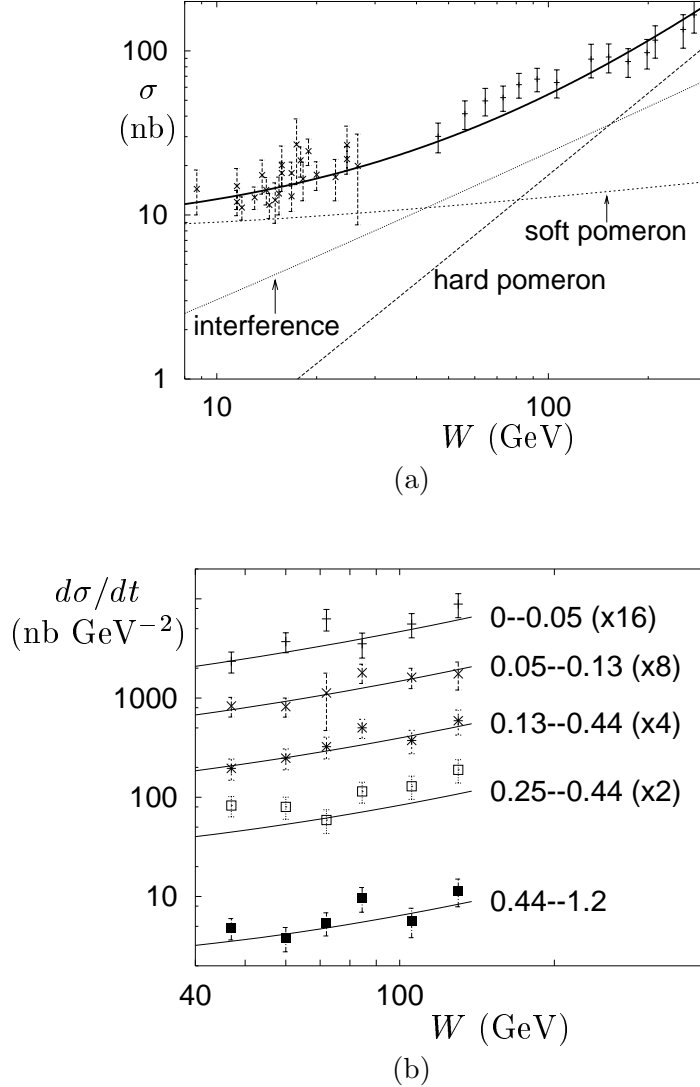


Figure 5: H1 data<sup>[8]</sup> for exclusive  $J/\psi$  production; (a) the total cross section and (b) the differential cross section for various ranges of  $t$ . The fits are described in the text.

We integrate  $d\sigma/dt$  calculated from (9) over  $t$  and fit to the total cross section for  $\gamma p \rightarrow J/\psi p$ , using the new H1 data and fixed-target data. The best fit gives

$$b_0 = 0.46 \quad b_1 = 5.4 \quad (13)$$

where the units are such that  $|A(s,t)|^2$  is the differential cross section  $d\sigma/dt$  in nb GeV<sup>-2</sup> units: see figure 5a. The data for  $d\sigma/dt$  are given in bins of  $t$ ; we average the  $|A(s,t)|^2$  over each bin, rather than simply evaluating it at the average value of  $t$  for the bin. The result is shown in figure 5b. Notice that, although neither pomeron has zero slope, the combined effect of the two pomerons has almost no shrinkage: the curves in figure 5b are rather parallel. One can understand how this comes about, because of our choice  $\alpha'_0 = 0.1$ . It is obvious that choosing the value  $\alpha'_0 = \alpha'_1 = 0.25$  would lead to shrinkage, while going to the limit  $\alpha'_0 = 0$  would produce negative shrinkage because as the energy increases the relatively-steep soft-pomeron term gives way to the flat hard-pomeron term.

**6** Regge theory should be applicable to larger values of  $x$  than 0.001, provided sufficient nonleading exchanges are included. For want of any proper information about these, and to avoid introducing

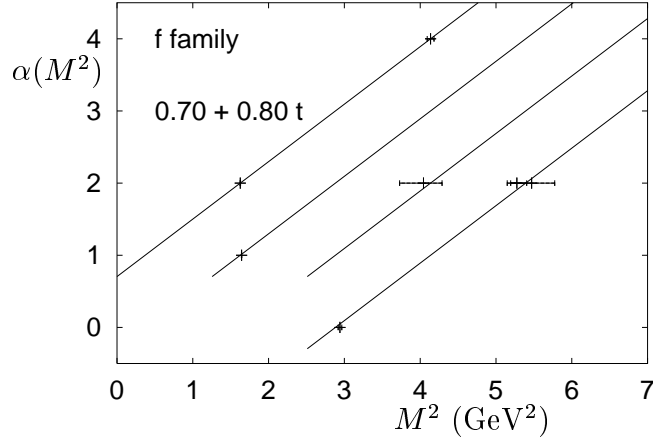


Figure 6: The  $f$  family of Regge trajectories

additional parameters, we have already said that we take them into account by including in each of the two pomeron terms a factor  $(1-x)^7$ , and in the  $(f_2, a_2)$ -exchange term a factor  $(1-x^2)^3$ . These powers agree with what the dimensional-counting rule would require for the behaviour as  $x \rightarrow 1$ ; we have no right to expect that such simple behaviour is correct away from  $x = 1$ , but it does work surprisingly well. In the Regge framework, the nonleading powers of  $x$  that we obtain when we multiply out these powers of  $(1-x)$  are interpreted as corresponding to the exchange of daughter trajectories. The concept of daughter trajectories was developed<sup>[14]</sup> at a time when little was known about meson spectroscopy, in order to cancel unwanted singularities in two-body nonelastic amplitudes such as  $\pi^- \pi^+ \rightarrow K^- K^+$ . This cancellation needs there to be an infinite sequence of daughter trajectories corresponding to each parent trajectory, with intercepts spaced one unit apart. If, as seems to be a good approximation, trajectories are straight, this implies that the existence of a particle of spin  $J$  implies that there also exist particles of spin  $J-1, J-2, \dots$  with the same mass and the same other quantum numbers as the parent particle. The data tables reveal the extensive existence of candidates for daughter particles; figure 6 shows the  $f$  family as an example. We assume that the two pomerons have daughters too. The theory tells us nothing about the  $Q^2$  dependence of the daughter contributions; our assumption that it is exactly the same as that of their parents is made to avoid having to introduce additional parameters and seems to work well.

**7** We saw in figure 1b that, according to the data, the shape of the soft-pomeron coefficient function  $f_1(Q^2)$  is sensitive to the value of the hard-pomeron power  $\epsilon_0$ . The value  $\epsilon_0 = 0.44$  gives a good fit to the data for  $x < 0.001$  with an  $f_1(Q^2)$  given in (4b), which goes to a constant at large  $Q^2$ . In our previous fit<sup>[1]</sup> we included also a factor  $(1 + Q/\bar{Q})^{-1}$  in (4b). If we do so now, and arbitrarily choose  $\bar{Q} = 10$  GeV, then the  $\chi^2$  per data point for the fit to the real-photon plus  $x < 0.001$  data changes only imperceptibly, and is still less than 1. It corresponds to the parameter values

$$\epsilon_0 = 0.3936 \quad X_0 = 0.002475 \quad Q_0^2 = 10.04 \quad X_1 = 0.5928 \quad Q_1^2 = 0.6643 \quad X_2 = 1.150 \quad Q_2^2 = 0.2603 \quad (14)$$

Choosing a yet smaller value for  $\bar{Q}$ , with correspondingly a smaller value for  $\epsilon_0$  still gives an acceptable fit.

**8** It is interesting to see how the fits compare with data at values of  $x$  larger than 0.001. There is no reason why they should perform well, because our simple choices of multiplicative factors  $(1-x)^7$  in the pomeron terms and  $(1-x^2)^3$  in the  $(f_2, a_2)$  term are surely too simple. Figure 7 shows the comparison with the data, for the parameter set (14). We emphasise that our fit used only data for  $x \leq 0.001$  and, as the parameters  $X_1$  and  $X_2$  were determined from the data for  $\sigma^{\gamma p}$ , only 5 parameters were adjusted to fit  $F_2(x, Q^2)$ .



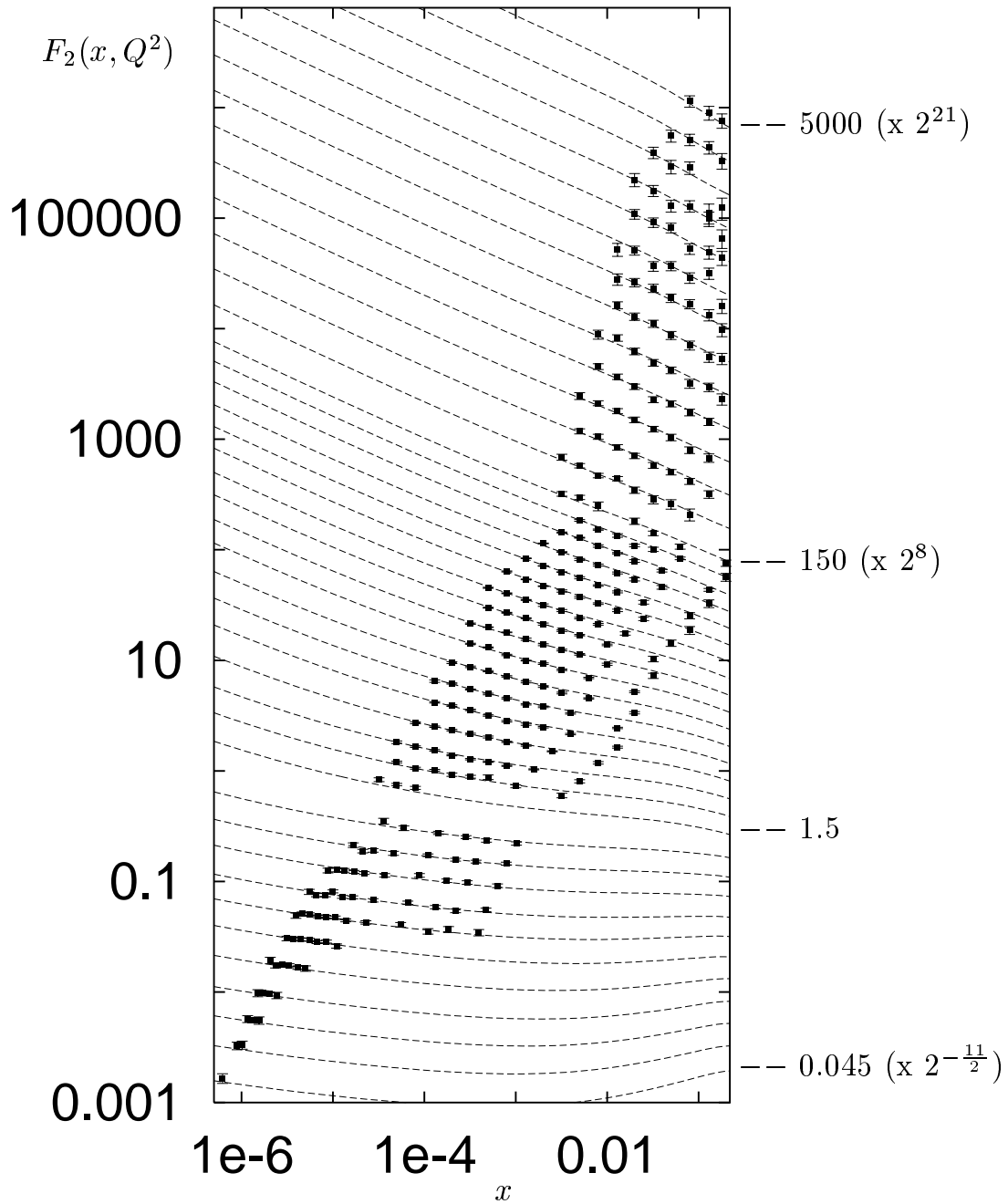


Figure 7: The fit described in the text compared with ZEUS and H1 data<sup>[6,7]</sup>. The data for the various  $Q^2$  values have been scaled with powers of  $\sqrt{2}$ , from  $Q^2 = 0.045$  GeV<sup>2</sup> at the bottom to 5000 GeV<sup>2</sup> at the top.

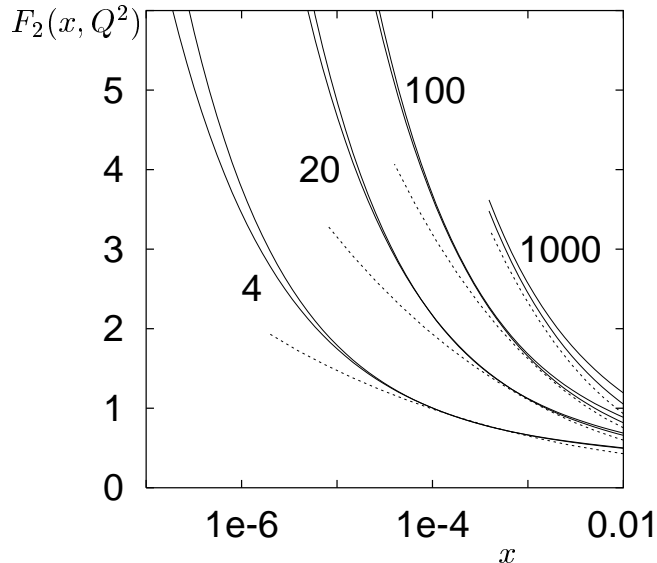


Figure 10: The solid lines compare the fits with the parameter sets (6) (upper curves) and (14) at various values of  $Q^2$ . The dashed curves are a two-loop pQCD fit<sup>[15]</sup>

**9** We have shown that the Regge approach to the data for the structure function  $F_2(x, Q^2)$  gives a very simple and remarkably successful description. There remains the urgent need to reconcile this approach with perturbative QCD, but that cannot be done so long as there is so little understanding of the theory of perturbative QCD at small  $x$ .

**10** We have seen that the error on the extraction of the value of the hard-pomeron intercept is quite large. Figure 10 illustrates this: the pairs of solid curves are for the two parameter sets (6) and (14), which have values of  $\epsilon_0$  differing by 10%. However, this figure shows that it may be possible to use LHC and THERA data to distinguish the Regge approach from the conventional DGLAP calculation with the splitting function calculated to fixed order in  $\alpha_s$ . The dashed curves show the result of such a fit<sup>[15]</sup> using a two-loop calculation\*. Perhaps not surprisingly, the Regge approach predicts that the rise at very small  $x$  is more rapid. It is often said that unitarity excludes such a rapid rise and forces it to be moderated by shadowing effects. However, while shadowing should eventually set in, there is no reliable way to estimate at what value of  $x$  it will occur, and unitarity gives no information. Unitarity places constraints of this type only on purely-hadronic amplitudes: there is no Froissart bound on  $\sigma^{\gamma p}$  or  $\sigma^{\gamma^* p}$ , because the unitarity equations are linear in the appropriate amplitudes.

---

\* We are grateful to Richard Ball for making available to us the numbers for the plot in his paper with Altarelli and Forte<sup>[15]</sup>

## References

- 1 A Donnachie and P V Landshoff, Physics Letters B437 (1998) 408
- 2 A Donnachie and P V Landshoff, Physics Letters B470 (1999) 243
- 3 A Donnachie and P V Landshoff, Physics Letters B478 (2000) 146
- 4 P D B Collins, *Introduction to Regge Theory and High Energy Physics*, Cambridge University Press (1977)
- 5 J R Cudell, A Donnachie and P V Landshoff, Physics Letters B448 (1999) 281
- 6 ZEUS collaboration: J Breitweg et al, Physics Letters B487 (2000) 53
- 7 H1 collaboration: C Adloff et al, hep-ex/0012052 and hep-ex/0012053
- 8 H1 collaboration: C Adloff et al, Physics Letters B483 (2000) 23
- 9 A Donnachie and P V Landshoff, Physics Letters B296 (1992) 227
- 10 J R Cudell et al, Physical Review D61 (2000) 034019; Erratum-*ibid* D63 (2001) 059901
- 11 ZEUS collaboration: J Breitweg et al, European Physical Journal C12 (2000) 35
- 12 J J Aubert et al, Nuclear Physics B293 (1987) 740
- 13 A Donnachie and P V Landshoff, Nuclear Physics B267 (1986) 690
- 14 D Z Freedman and J M Wang, Physical Review 153 (1967) 1596
- 15 G Altarelli, R D Ball and S Forte, hep-ph/0104246